

Chapter 7: Properties of Turbulent Free Shear Flow (Chap. 11 Bernard)

Part 4: Turbulent Mixing Layer

Two parallel fluid streams with different mean velocities are brought together at a sufficiently high Re .



$$\begin{aligned} U_l &< U_u \\ \frac{U_l}{U_u} &= 0.38 \end{aligned}$$

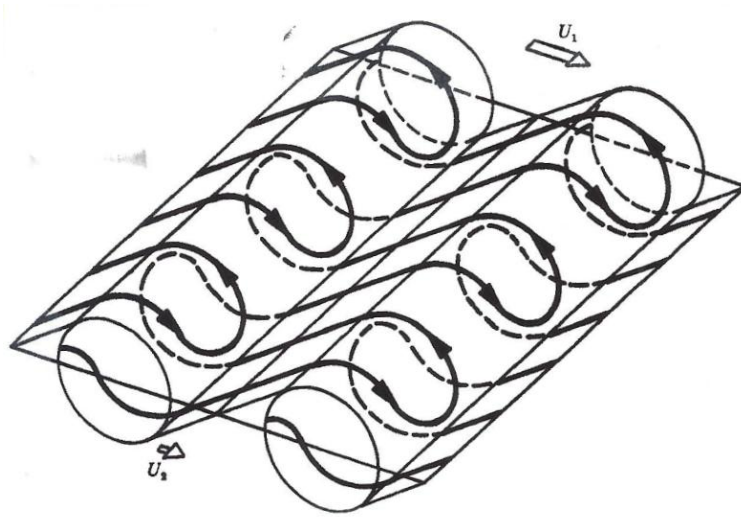
Figure 11.9 Growth of a turbulent mixing layer with x , y , and z denoting the streamwise, cross-stream, and spanwise coordinates, respectively. Top: viewed from above ($x - z$) plane; bottom: viewed from the side ($x - y$) plane. From [15].

$Re_\omega = 6500$, i.e., based on vorticity thickness $\Delta U / (d\bar{U}/dy)_{max}$ is condition for transition to fully turbulent flow.

Kelvin-Helmholtz interface instability with spanwise rollers, which grow as they convect downstream by ingesting the external irrotational flow. Irregular motions within roller exhibit the turbulence. Pairing of the rollers occurs when two adjacent rollers merge into single larger vortex.

Mixing layer turbulence and roller size grow linearly. Coherent roller structures persist at large distances.

Top view shows another coherent structure, i.e., streamwise rib vortices, which wrap around (braid) the rolling vortices.



Braiding of rib and roller vortices

FIGURE 15. Topology of streamwise vortex lines.

11.10 Formation of interaction rollers and rib vortices

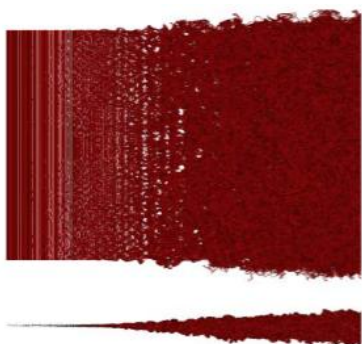
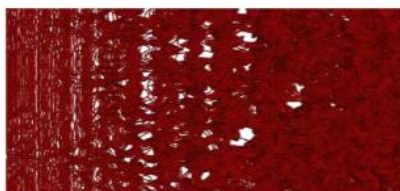


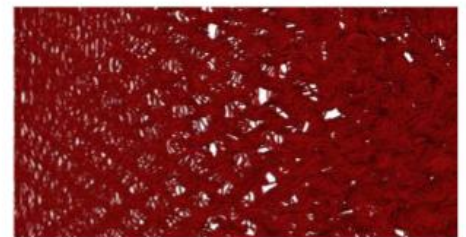
Figure 11.10 Overhead (top) and side (lower) views of a vortex filament computation of a mixing layer [22]. Used by permission of AIAA.



FLOW →

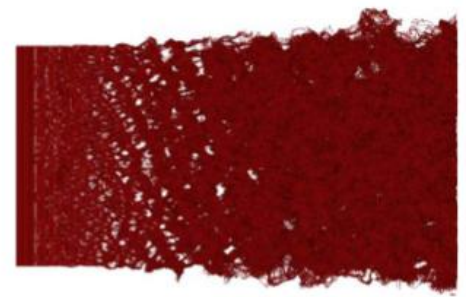
FLOW →

Figure 11.12 Detail of a chain-link fence vortex pattern developing in a vortex filament simulation of a mixing layer [22]. Used by permission of AIAA.



FLOW →

Figure 11.13 Overhead view of a mixing layer containing oblique roller/braid vortices.



FLOW →

Close up 3D view of transition to turbulence as roller + rib vortices interact.

Self-Preserving Mixing Layer

Recall BL streamwise momentum equation:

$$\bar{U} \frac{\partial \bar{U}}{\partial x} + \bar{V} \frac{\partial \bar{U}}{\partial y} + \frac{\partial \bar{u}\bar{v}}{\partial y} = 0 \quad (1)$$

For a mixing layer U_l and U_u are uniform mean velocities on low and high-speed sides. Comparing with wake scaling where $\Delta U = U_e - \bar{U}_{min}(x)$ and jet flow where $\Delta U = \bar{U}_{max}(x)$, for mixing layers $\Delta U = U_u - U_l$. Therefore, the form of the stream function is:

$$\bar{\Psi} = l(x)U_m F(\eta)$$

Where:

$$U_m = \frac{(U_u + U_l)}{2}$$

And $\eta = y/l(x)$ is the similarity variable.

Recall relation between \bar{U} , \bar{V} and $\bar{\Psi}$:

$$\bar{U} = \bar{\Psi}_y \quad (2)$$

$$\bar{V} = -\bar{\Psi}_x \quad (3)$$

Such that:

$$\bar{U} = lU_m \frac{dF(\eta)}{d\eta} \frac{d\eta}{dy} = U_m F' \quad (4)$$

$$\bar{V} = -\frac{dl}{dx} U_m F(\eta) - lU_m \frac{dF(\eta)}{d\eta} \frac{d\eta}{dx}$$

$$\frac{d\eta}{dy} = \frac{d\left(\frac{y}{l}\right)}{dy} = \frac{1}{l}$$

$$\begin{aligned} \frac{d\eta}{dx} &= \frac{d\left(\frac{y}{l}\right)}{dx} \\ &= -\frac{y}{l^2} \frac{dl}{dx} = -\frac{\eta}{l} \frac{dl}{dx} \end{aligned}$$

$$\bar{V} = -\frac{dl}{dx} U_m F(\eta) + \eta U_m F' \frac{dl}{dx} \quad (5)$$

Differentiating Eq. (4) with respect to x yields:

$$\frac{\partial \bar{U}}{\partial x} = U_m \frac{dF'}{d\eta} \frac{d\eta}{dx} = -\frac{\eta}{l} U_m F'' \frac{dl}{dx} \quad (6)$$

Similarly, differentiating with respect to y gives:

$$\frac{\partial \bar{U}}{\partial y} = U_m \frac{dF'}{d\eta} \frac{d\eta}{dy} = \frac{U_m}{l} F'' \quad (7)$$

Assuming:

$$\bar{uv} = -U_m^2 g(\eta) \quad (8)$$

$$\frac{\partial \bar{uv}}{\partial y} = -U_m^2 \frac{dg(\eta)}{d\eta} \frac{d\eta}{dy} = -\frac{U_m^2}{l} g' \quad (9)$$

And combining Eqs. (4), (5), (6), (7) and (9) into Eq. (1) gives:

$$\begin{aligned} -F' \frac{\eta}{l} U_m^2 F'' \frac{dl}{dx} + \left(-\frac{dl}{dx} U_m F + \eta U_m F' \frac{dl}{dx} \right) \frac{U_m}{l} F'' - \frac{U_m^2}{l} g' &= 0 \\ \cancel{-F' \frac{\eta}{l} U_m^2 F'' \frac{dl}{dx}} - \frac{dl}{dx} \frac{U_m^2}{l} F F'' + \cancel{F' \frac{\eta}{l} U_m^2 F'' \frac{dl}{dx}} &= \frac{U_m^2}{l} g' \end{aligned}$$

Divide by U_m^2/l :

$$\frac{dl}{dx} FF'' + g' = 0 \quad (10)$$

Eq. (10) implies that for a similarity solution to exist,

$$l(x) = \alpha(x - x_0) \rightarrow \frac{dl}{dx} = \alpha$$

Where α is a constant.

Assuming eddy viscosity model:

$$\begin{aligned} \overline{uv} &= -\nu_t \frac{\partial \bar{U}}{\partial y} = -\nu_t \frac{U_m}{l} F'' \\ \frac{\partial \overline{uv}}{\partial y} &= -\nu_t \frac{U_m}{l} \frac{dF''}{d\eta} \frac{d\eta}{dy} = -\nu_t \frac{U_m}{l^2} F''' = -\frac{U_m^2}{l} g' \end{aligned}$$

i.e.,

$$g' = \frac{\nu_t}{U_m l} F''' = \frac{F'''}{R_t}$$

$$R_t = \frac{U_m l(x)}{\nu_t}$$

Such that Eq. (10) becomes:

$$\alpha R_t FF'' + F''' = 0 \quad (11)$$

Where R_t must be constant to maintain similarity, i.e., $\nu_t \propto x$.

BCs for Eq. (11) are:

$$\bar{U}(x, +\infty) = U_u \rightarrow F'(+\infty) = \frac{U_u}{U_m} = \frac{2U_u}{U_u + U_l}$$

$$F'(+\infty) = \frac{U_u + U_l}{U_u + U_l} + \frac{U_u - U_l}{U_u + U_l} = 1 + \frac{\Delta U}{2U_m} = 1 + \lambda$$

$$F'(+\infty) = 1 + \lambda$$

Where:

$$\lambda = \frac{\Delta U}{2U_m} = \frac{U_u - U_l}{U_u + U_l}$$

and

$$\Delta U = U_u - U_l$$

Similarly, for

$$\overline{U}(x, -\infty) = U_l \rightarrow F'(-\infty) = 1 - \lambda$$

Eq. (11) is identical to classical Blasius BL equation for zero-pressure gradient BL. As in the case of BL flow, Eq. (11) does not have closed form solution. However, it is possible to assume a power series solution for small λ :

$$F(\eta) = \eta + \lambda F_1(\eta) + \lambda^2 F_2(\eta) + \dots \quad (12)$$

Where the functions $F_n = F_n(\eta)$ need to be determined.

Recall:

$$\overline{U} = U_m F' \quad (4)$$

The first term in the series can be deduced: at $\eta = 0$, $\overline{U}(0) = U_m \rightarrow F'(0) = 1$ and integrating $F(0) = \eta$, which represents the first term in the series.

And substituting power series solution of $F(\eta)$ gives:

$$\overline{U} = U_m F' = U_m + U_m \lambda F'_1(\eta) + U_m \lambda^2 F'_2(\eta) + \dots \quad (13)$$

Substituting Eq. (12) into Eq. (11) gives:

$$\alpha R_t (\eta + \lambda F_1(\eta) + \lambda^2 F_2(\eta)) (\lambda F_1''(\eta) + \lambda^2 F_2''(\eta)) + \lambda F_1'''(\eta) + \lambda^2 F_2'''(\eta) = 0$$

And collecting terms according to powers of λ :

$$1^{\text{st}} \text{ order: } \alpha R_t \eta F_1''(\eta) + F_1'''(\eta) = 0$$

$$F_1''(\eta) = C e^{-\frac{\alpha R_t \eta^2}{2}}$$

The arbitrary constant α can be picked such that $\alpha R_t = 2$. Therefore,

$$\eta = \frac{y}{l(x)} = \frac{y}{\alpha(x - x_0)} = \frac{R_t}{2} \frac{y}{(x - x_0)}$$

And

$$F_1''(\eta) = C e^{-\eta^2} \quad (14)$$

If $F(\eta)$ is truncated to 1st order:

$$F(\eta) = \eta + \lambda F_1(\eta)$$

The BCs $F'(\pm\infty) = 1 \pm \lambda$ imply that:

$$F_1'(\pm\infty) = \pm 1 \quad (15)$$

Integrating Eq. (14) and applying Eq. (15) gives

$$F_1' = \operatorname{erf} \eta$$

Where:

$$\operatorname{erf} \eta = \frac{2}{\sqrt{\pi}} \int_0^\eta e^{-\xi^2} d\xi$$

is the error function. Finally, truncating Eq. (13) to 1st order gives:

$$\bar{U} \approx U_m (1 + \lambda F_1'(\eta)) = U_m \left(1 + \frac{\Delta U}{2U_m} \operatorname{erf} \eta \right) \quad (16)$$

The only parameter left is $R_t = f(U_u/U_l) \approx 27$ which is typical value from EFD.

Alternative definition of momentum thickness for mixing layers is given by:

$$\rho \theta (\Delta U)^2 = \rho \int_{-\infty}^{\infty} (U_u - \bar{U})(\bar{U} - U_l) dy \quad (17)$$

RHS = Momentum deficit (in relation to U_u) in the flux of momentum measured relative to U_l .

θ = thickness of a layer due to momentum defect at speed U_u with flux relative to U_l .

Substituting Eq. (16) into (17) shows that:

$$\frac{\theta}{l} = \frac{1}{4} \int_{-\infty}^{\infty} (1 - \operatorname{erf}^2 \eta) d\eta$$

or

$$\theta \sim l = \alpha(x - x_0)$$

Growth rate parameter:

$$r_\theta = \frac{U_m}{\Delta U} \frac{d\theta}{dx}$$

is a universal constant.

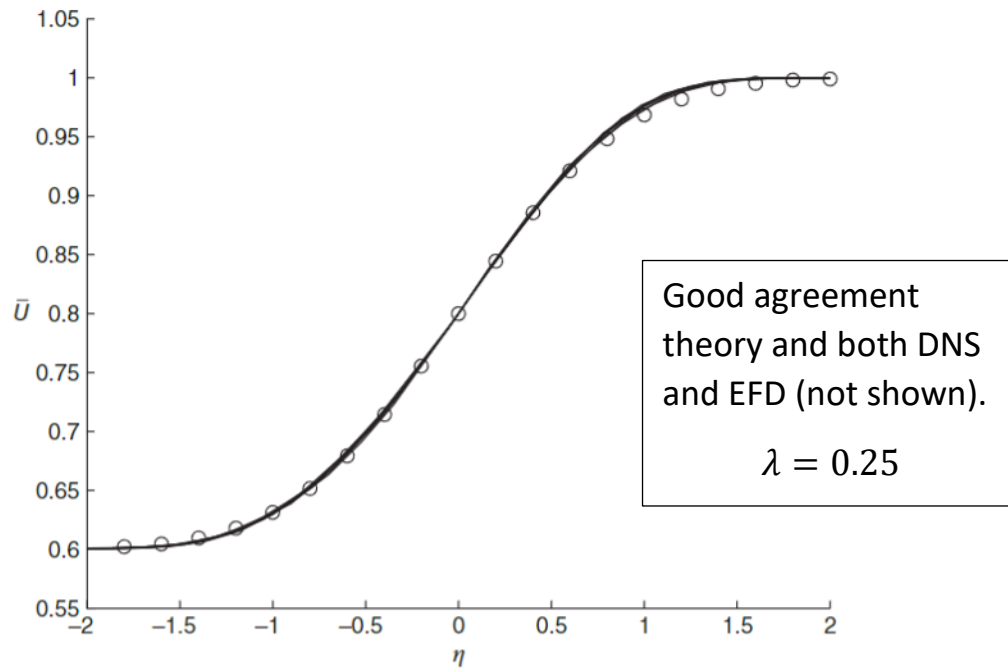


Figure 11.14 Mean streamwise velocity distributions in a self-preserving two-stream mixing layer. Solid lines are results from seven locations across a vortex filament simulation of a mixing layer ([22]). o, Eq. (11.88). Used by permission of AIAA.

Reynolds stresses: EFD and DNS with $\eta = y/\theta$.

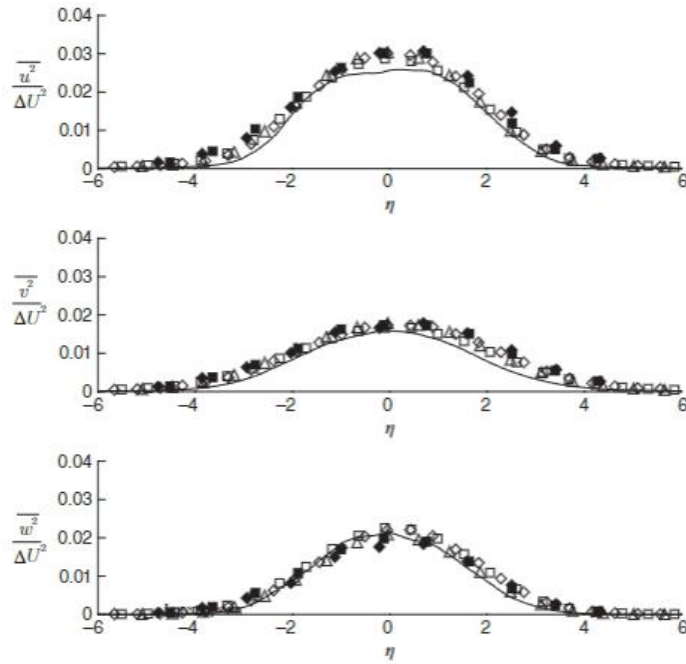
$$\overline{u_i u_j}|_{max} \rightarrow \eta = 0$$

where \bar{U} has inflection point.

$$\overline{u^2} > \overline{w^2} > \overline{v^2}$$

uv also shows self-similarity.

$v_t \sim \text{constant } \eta \leq \pm 3$.



Max at $\eta = 0$
where \bar{U} has
inflection point,
max gradient \bar{U}_y

Figure 11.15 Normal Reynolds stresses in a two-stream mixing layer. Here, $\eta = y/\theta$. Experiment [25]: \blacklozenge , $R_\theta = 1,792$; \blacksquare , $R_\theta = 2,483$. Experiment [26]: \square , $R_\theta \approx 3,820$; \diamond , $R_\theta \approx 4,380$; \triangle , $R_\theta \approx 6,365$. DNS [21]: —, averaged for $R_\theta = 1,500$ – $2,000$.

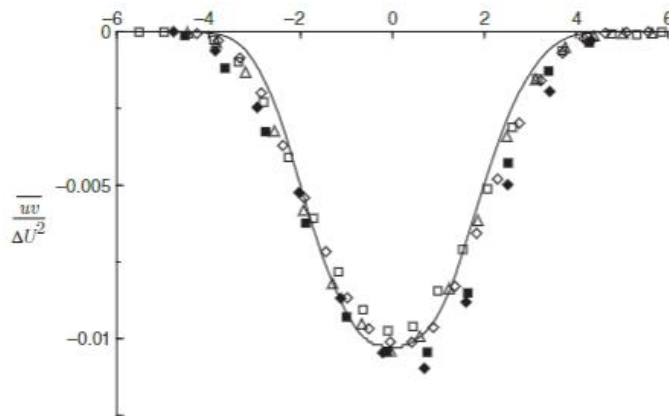


Figure 11.16 Reynolds shear stress distributions in a two-stream mixing layer. Here, $\eta = y/\theta$. Symbols as in Figure 11.15.